Environmental Science & Technology

ACS AuthorChoice

Article

Cite This: Environ. Sci. Technol. 2018, 52, 10134−10143

pubs.acs.org/est

# Mixing State of Carbonaceous Aerosols of Primary Emissions from "Improved" African Cookstoves

Yuchieh Ting,[†] Edward J. S. Mitchell,[‡] James D. Allan,[*,†,§] Dantong Liu,[†] Dominick V. Spracklen,[∥] Alan Williams,[‡] Jenny M. Jones,[‡] Amanda R. Lea-Langton,[⊥] Gordon McFiggans,[†] and Hugh Coe[†]

[†]School of Earth and Environmental Science, University of Manchester, Manchester M13 9PL, United Kingdom

[‡]School of Chemical and Process Engineering, University of Leeds, Leeds LS2 9JT, United Kingdom

[§]National Centre for Atmospheric Science, University of Manchester, Manchester M13 9PL, United Kingdom

[∥]School of Earth and Environment, University of Leeds, Leeds LS2 9JT, United Kingdom

[⊥]School of Mechanical, Aerospace and Civil Engineering, University of Manchester, Manchester M13 9PL, United Kingdom

Supporting Information

**ABSTRACT:** Designs of "improved" stoves are introduced recently to benefit the solid fuel consumption of cooking activities in developing countries, but the uncertainties concerning the combustion processes and particulate emissions remain poorly characterized. To help understand this, combustion in three examples of "improved" African cookstoves was investigated in the laboratory. A typical European heating stove was included for comparison purpose. Detailed aerosol emissions were studied in real-time with an Aerosol Mass Spectrometer and Single Particle Soot Photometer, to explore interactions between black carbon (BC) and organic carbon aerosols, which were parametrized according to modified combustion efficiency (MCE), a common metric used within the atmospheric emission community. Greater than 50% of the total organic matter (OM) was found in BC-containing particles when MCE was >0.95 for dry oak and coal fuels, whereas at lower MCE, over 80% of the total OM for most of the fuels existed in particles without detectable BC. When the OM mass fraction of total particulate matter ($PM_1$) > 0.9, the mass ratio of OM to refractory BC in BC-containing particles was about 2−3, but only ∼0.8 when OM mass fraction <0.9. These findings are not currently included in models and such information should be considered in the future emission scenarios.

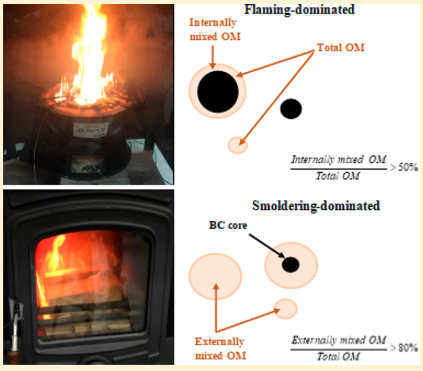


## INTRODUCTION

Particulate emissions from the combustion of solid fuel, which is widely used for cooking and heating in developing countries, have severe impacts on human health, air quality, and climate.[1−4] For the year 2010, global burden of disease estimates showed that exposure to household air pollution from cooking resulted in approximately 4 million premature deaths,[5] with the most recent estimates from WHO reporting 4.3 million death for 2012.[6] Household air pollution is also a substantial contributor to outdoor air pollution-related deaths due to emissions into the ambient environment, responsible for around 0.4 million deaths (12%) of the total from ambient air pollution.[7]

Domestic combustion of solid fuels was estimated to contribute to approximate 30% and 70% of global BC and organic carbon (OC) emissions, respectively,[8] although there were big regional differences depending on the operating conditions such as fuel type, appliance type, and fuel loading, which can influence emission compositions considerably.[9−13] BC is the dominant form of light absorbing particulate matter and is estimated to be the most important anthropogenic contributor to instantaneous climate forcing after $CO_2$.[11] Co-emitted OM also affects the optical properties of emitted BC particles if the components are internally mixed, through coatings and lensing effects.[14−16]

The chemical composition of stove-related combustion emissions was found to vary widely and depend on the fuel type, source loading, and condition, all of which affect combustion conditions.[17−21] Further variations may be expected with the introduction of new technologies designed to reduce fuel consumption and emissions, where the improved combustion efficiency may change the character of the emissions, in addition to the quantity.

Although there have been a number of studies using real-time instrumentation to characterize solid fuel combustion emissions from heating and cooking stoves, most of them focused on particle number concentrations,[22−26] OM composition,[12,13,27−29] and the characterization of BC.[28,30−32] The information about real time emissions of BC and OM and

Received: January 25, 2018
Revised: July 27, 2018
Accepted: August 1, 2018
Published: August 1, 2018






DOI: 10.1021/acs.est.8b00456
Environ. Sci. Technol. 2018, 52, 10134−10143

how they are mixed with each other is still lacking.[33,34] The absorption enhancement of BC particles is determined by the mixing state of BC and non-BC materials in a BC-containing particle[14,16,35,36] but this is still uncertain, particularly for solid fuel emissions, and is often largely simplified in models.[37,38] Thus, the unconstrained source profiles of solid fuel emissions limit the ability to accurately simulate the impacts on air quality and climate.[3] The relationship between the emissions from solid fuel combustion and combustion efficiency has been shown in a few studies, but many of the tests were conducted on more idealized and tightly constrained combustion conditions and hence were unable to replicate the diversity of emissions.[10,12,32]

The burning conditions and emissions of the stoves are highly variable and stove performance in the field can be quite different from that in the laboratory.[39−41] While integrated emissions are of use to inform inventories,[42−44] to better understand the exact nature of the emissions, it is important to make high time-resolution measurements of the entire process to have an insight into the evolution of the properties of the emissions. Furthermore, the use of the same type of online instrumentation for emissions and atmospheric measurements enables direct comparison of data sets. In this study, the chemical compositions of nonrefractory species in $PM_1$ were measured by a compact time-of-flight aerosol mass spectrometer (c-TOF-AMS), and the physical properties of refractory BC (rBC) particles were characterized by using a single particle soot photometer (SP2). The mixing state of rBC and coemitted OM components emitted from the cookstoves was reported and compared to those emitted from a UK heating stove, and their relationships to the MCE and the oxidation level of the emissions, which potentially affects the BC particles, were qualitatively provided for comparability to equivalent atmospheric measurements of air pollutants from wood combustion. To our knowledge, this is the first time to explore the mixing state between OM and BC from solid fuel combustion from both stove types as sources.

## MATERIALS AND METHODS

**Testing Facility and Combustion Experiments.** A series of solid fuel combustion experiments was carried out in the test facility of the University of Leeds. The facility was modified for cookstove testing having been previously used for heating stoves testing.[45] Details of this facility, including the stoves, types of fuel used, and sampling configuration are in the Supporting Information (SI Figures S1 and S2, and Table S1). Three examples of cookstoves used in Africa that could be described as "improved" (better fuel efficiency and lower emissions compared to the traditional cookstoves, such as three stone fires) were used and are named here as Carbonzero,[46] Gyapa,[47] and Lucia.[48] For the sake of comparison, a modern U.K. heating stove[49] was also tested. It should be noted that cookstoves were tested with no cooking pot, which can have a large effect on performance by changing air flow and by quenching flames and combustion gases.

For each combustion experiment except for the Lucia stove, standard ZIP firelighters (http://www.zipfires.co.uk/product-range/fire-lighters/high-performance/) were used to ignite the fuel, which caused ignition of the firelighter immediately and pyrolysis of the solid fuel before consequent burning. Fuel was reloaded manually when the flame on the top of the burning fuel almost died out while the combustion process was ongoing, as would be performed during normal operation. The Lucia stove was a pyrolytic stove with a fundamentally different combustion mechanism. Fuel pellets are pyrolyzed and the resultant gases driven through an outer sheath before combustion at a ring of holes above the fuel bed. The pyrolysis and flow are maintained passively by the heat of the flame, and the initial ignition was provided by 9 g of liquid kerosene.

Different studies have the distinct definitions of the burning phases.[12,23,27,29,50] In this study, the burns for each stove can be qualitatively divided into several phases according to the observed variability of burning conditions and particulate emissions. Typically, these were (i) "fuel reloading", which started when fuel was reloaded on the glowing embers of the proceeding combustion cycle. This included the pyrolysis phase and lasted until BC and the modified combustion efficiency (MCE), calculated as $\Delta CO_2/(\Delta CO + \Delta CO_2)$, increased; (ii) "flaming-dominated", that followed the initial phase of fuel addition and lasted until the MCE and BC emissions dropped; (iii) "poor-burning", which was characterized by a lack of significant dominance in the OM and BC emissions with the fluctuation in MCE over several combustion cycles; (iv) "smoldering-dominated", that occurred only in the combustion cycle with charcoal and coal in this study, during this phase OM emissions were elevated with only nominal BC and little visible flame; and (v) "burn out", which was only observed significantly for the Lucia stove.

**Instrumentation and Data Analysis.** A cToF-AMS was used for the online measurement of submicron nonrefractory aerosol components, including OM, nitrate ($NO_3^-$), sulfate ($SO_4^{2-}$), ammonium ($NH_4^+$), and chloride ($Cl^-$). The operating modes of the AMS and detailed descriptions of the cToF-AMS can be found in other publications.[51,52] Details of the data processing and the correction of the mass spectra are in the SI.

The physical and optical properties of individual rBC particles were characterized by a SP2 manufactured by Droplet Measurement Technology (DMT). The operation and data analysis procedures of the SP2 used in these experiments have been described in McMeeking et al.[53] and Liu et al.[54] The SP2 uses incandescence induced by a 1064 nm active laser cavity to obtain rBC mass in individual particles which can be converted to a sphere-equivalent core diameter (Dc) by assuming a density of 1.8 g $cm^{-3}$.[55] This is done for the sake of comparison with other sizing instruments. A further estimate of overall size can also be provided by inspecting the scattering signal as the particle enters the laser beam, using the "leading edge only" method described by Liu et al.[56] and Taylor et al.[57] A core−shell Mie model was used, assuming a rBC core refractive index of 2.26−1.26i and a coating refractive index of 1.5 + 0i.[58] While it would have been preferable to derive refractive indexes specific to these aerosol, this was not possible with the equipment used here.

The SP2 data were used to estimate the mass of the non-BC material coating on the BC particles from the total volume of the BC particles divided by the total volume of the BC cores as measured within a given time period,[56] as expressed as eq 1. The non-BC material of a BC-containing particle is deemed to be mostly consisted of OM internally mixed with BC. The total organic mass internally mixed with BC in a given time period, $OM_{BC}$, can then be obtained using the bulk $V_P/V_C$ by assuming the densities of OM and BC as expressed by eq 2:


DOI: 10.1021/acs.est.8b00456
Environ. Sci. Technol. 2018, 52, 10134−10143

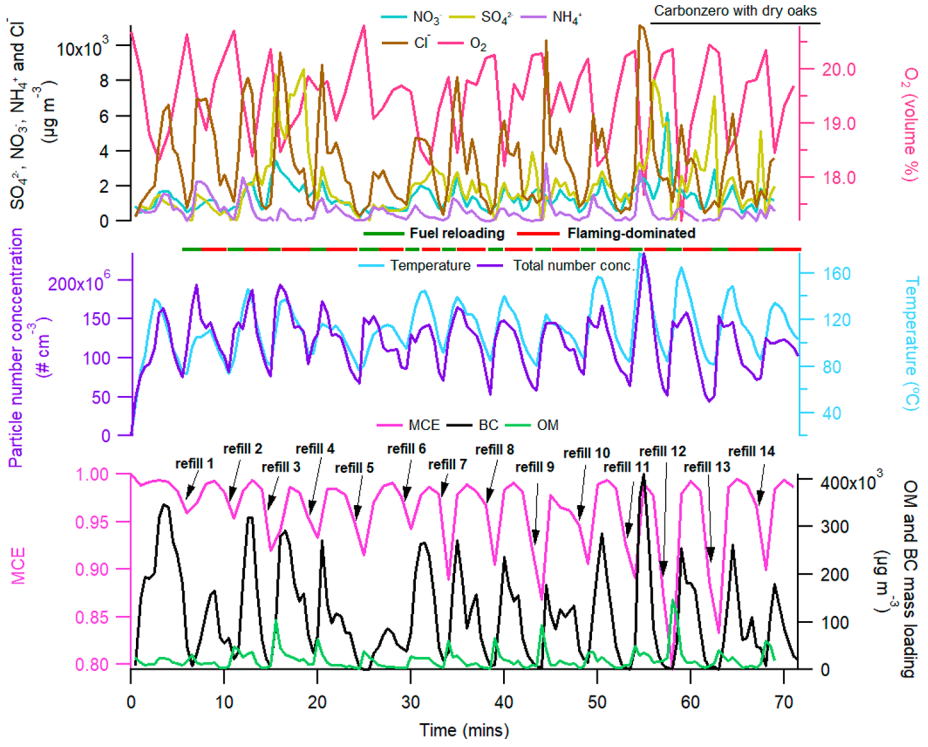


**Figure 1.** Time series of inorganic aerosol ($SO_4^{2-}$, $NO_3^-$, $NH_4^+$, and $Cl^-$) concentrations, oxygen volume concentrations, the particle number concentrations, temperature of the flue, modified combustion efficiency (MCE), OM, and BC mass concentrations for an experiment (in this case dry oak using Carbonzero stove), with the timing of refilling the fuels and an indication of the defined burning phases.

$$\frac{V_P}{V_C} = \left(\frac{\sum_i D_{P,i}^3}{\sum_i D_{C,i}^3}\right) \quad (1)$$

$$OM_{BC} = \frac{\left(\frac{V_P}{V_C} - 1\right)}{\rho_{BC}} \times \rho_{OM} \times \sum_i rBC_i \quad (2)$$

where $\rho_{OM}$ and $\rho_{BC}$ are the densities of OM and BC assumed to be 1.2 and 1.8 g cm$^{-3}$, respectively,[55,59] and $\sum_i rBC_i$ is the total mass of black carbon in a population of $i$ particles, which we later term $rBC_{bulk}$. A fraction of particles with small BC cores and thin coatings may not be detected by the SP2, though this fraction of coating mass was of minor importance (~5−10%) considering the total coating mass. While it is noted that this method carries uncertainties relating to assumptions concerning shape, density, and refractive index, this still serves as a good comparative metric between stoves and fuels. The lower detection limit of the BC core size from the SP2 is a mass corresponding to around 60 nm diameter.[35] This precludes the ability to identify particles as completely BC-free, i.e., externally mixed with BC, since they can contain some fraction of rBC below the SP2 detection limit (<60 nm). As the mass of the BC emissions from charcoal combustion was too low, this approach was not applicable to the estimation of the coatings in the charcoal experiment.

Given that the AMS is able to detect total OM, the internally mixed OM fraction relative to total OM, denoted as $F_{in}$, can be obtained by eq 3:

$$F_{in} = \frac{OM_{BC}}{OM_{total}} \quad (3)$$

where $OM_{BC}$ is the OM internally mixed with BC determined by the SP2 measurement, $OM_{total}$ is the total OM measured by the AMS.

The number concentrations and size distribution of submicron particles were measured by a fast response differential mobility spectrometer (DMS500, Cambustion Ltd., Cambridge, U.K.). The soot calibration was performed using a bimodal agglomerate matrix to invert the data.[60] Gaseous emissions in the flue were measured by a Gasmet Dx-4000 Fourier Transform Infrared (FTIR) spectrometer (Temet Instruments OY, Finland) before the second stage dilution and by a Testo 340 analyzer (Testo INC, Lenzkirch, Germany) after the second stage dilution (Figure S1). A number of thermocouples were deployed to measure the temperatures of the flue gas and different positions of the firebox. Two Dekati dilutors (DI-1000, Dekati Ltd., Finland) were placed in series before the AMS and SP2 measurement, giving a third stage of dilution with compressed air (Figure S1). The dilution ratio was nominally set to 100, although this was subsequently found to vary as material collected on the first stage nozzle over the course of the experiment. Due to this and the uncontrolled nature of the dilution from the flue to the extraction tunnel, the dilution factor was derived by comparing the total particle volume derived by the DMS500 (from the flue) measurement and that obtained by the AMS and SP2 (after the two-stage dilutor) (Figure S3). This was applied to obtain the undiluted concentrations. To investigate the relationships between combustion conditions and emissions, the MCE was used to indicate the efficiency of the burn, in keeping with various atmospheric emission studies;[10,13,61−63] however, recent studies on the highly controlled combustion of small wood samples have suggested this may be overly simplistic,[32] as the pyrolysis emissions that occur prior to the


DOI: 10.1021/acs.est.8b00456
Environ. Sci. Technol. 2018, 52, 10134−10143

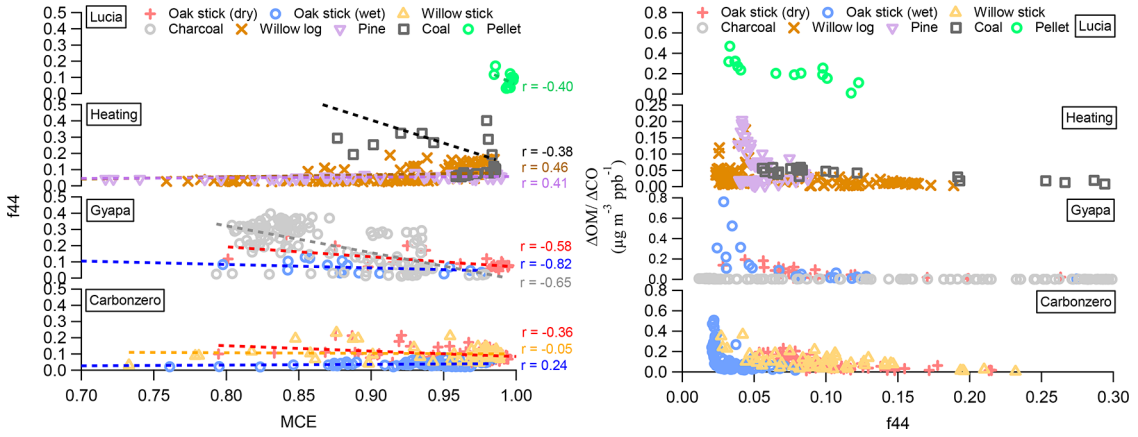


**Figure 2.** *f44* versus MCE for each combustion cycle (left panel). ΔOM/ΔCO versus *f44* for each combustion cycle (right panel).

local ignition of the fuel may be very significant. The temperature and oxygen measured in the flue were also used as references for combustion conditions. The data from all instruments were averaged to 1 min for the convenience of intercomparison between the different measurements.

The emission ratios (ER) of number concentration of particles with aerodynamic diameter less than 1 $\mu$m ($PN_1$), $PM_1$ (organics, inorganics and black carbon), OM and BC are normalized to excess CO (i.e., ERx = ΔX/ΔCO, X is the emitted species) to track the relative abundance of the species. The data were not used in this analysis if the OM or BC concentrations were lower than 0.04 $\mu$g $m^{-3}$ as the low number included in the coating calculation introduced a large uncertainty. BC mass loadings from charcoal combustion emissions were below 0.04 $\mu$g $m^{-3}$ for most of the time and are thus not included in the data analysis.

## RESULTS

**Real-Time Measurements Resolving Burning Cycle.** Figure 1 shows an example of one experiment demonstrating the time series of emissions during burning phases with sequential addition of fuel. The other experiments are shown in SI Figure S4.

As Figure 1 shows, for each burning cycle, OM emissions peaked immediately after fuel addition, which in general correlated with a lower MCE and may be mainly from the pyrolysis process followed by the flaming-dominated phase with a high MCE, consistent with Haslett et al.[32] BC and inorganic particle components peaked at high MCE and temperature, and the MCE dropped each time the fuel refilled as more charcoal accumulated. The non-BC inorganic components ($SO_4^{2-}$, $NO_3^-$, and $NH_4^+$) only contributed to a small mass fraction of the total PM (~5−10%).

There were some differences in other combustion cycles, shown in Figure S4, depending on the fuel and stove used. In the charcoal combustion experiments, the smoldering phase continued through most of the burning cycle and gave dominant emissions of OM and minimum BC. The emissions from solid fuel combustion in the heating stove showed different features, and in most cases, it was not possible to distinguish the burning phases. With the pellet combustion using the Lucia stove, a high correlation between the OM and BC was observed, indicating that pyrolysis and flaming overlapped during the combustion cycle. In addition, the Lucia stove combustion showed a good performance with stable high MCE and produced a relatively lower proportion of OM compared to the others.

Measurements of the number size distribution of dry fuels show a bimodal distribution, whereas that of wet fuels was unimodal (Figure S5(a)). The two dry fuel modes may well arise from different burn phases. The average BC core size distribution are very consistent between the different burns (Figure S5(b)).

Figure S6 illustrates the general decreasing trend of OM mass fraction in total carbonaceous particles OM/(OM + BC) with increasing MCE for all combustions. Apart from the heating stove with coal and Gyapa with dry and wet oaks, the fraction of organic to total carbonaceous species was almost unity for MCE < 0.85. For most of the fuels (apart from pine), the OM fraction started to drop substantially when MCE > 0.85, reducing to around 0.1 when MCE was close to 1. This indicates that above a critical point of MCE, the combustion started to emit a significant amount of BC compared to OM, but below this MCE threshold the OM fraction tended to be higher for most of the fuels but also depended on the stove types. Considering all combustions, at a given MCE, a large variation in OM fraction was observed across the range of different stoves and fuels. This means a single parameter of OM fraction or MCE is unable to fully describe the burning phases in the real world. For this reason, this study uses the MCE as the reference parameter for emission characterization, but does not attempt to unambiguously identify burning phases.

**Oxygenation of OM.** The degree of oxygenation of OM, as indicated by the fraction of $m/z$ 44 ($CO_2^+$) in the total organic mass spectra (*f44*),[64] was evaluated against MCE and the ER of OM. For the measurements of OM compositions at the source, changes in *f44* are more likely to reflect the effects of combustion processes rather than subsequent oxidation because of the short aging time involved. However, not only the combustion efficiency, but also the stove types, fuel species, and moisture content may cause the varying *f44*. The correlation between *f44* and MCE, shown in Figure 2 (left panel), appears to be highly dependent on both stove and fuel type. For the dry oak fuel in the Carbonzero and Gyapa cookstoves, the correlations between *f44* and MCE were negative ($r$ = −0.36 and −0.58). However, for the wet oak in the Carbonzero cookstove, the positive correlation was weak ($r$ = 0.24), whereas in the Gyapa stove, a high negative correlation ($r$ = −0.82) was observed. For the combustion cycles in the heating stove, the relationship between *f44* and


DOI: 10.1021/acs.est.8b00456
Environ. Sci. Technol. 2018, 52, 10134−10143

MCE showed dependence on fuel type with a positive correlation for willow log and pine ($r$ = 0.46 and 0.41, respectively), whereas a negative correlation was observed for coal ($r$ = −0.38).

Despite the limited dependence upon the MCE, *f44* reveals a notable relationship with ΔOM/ΔCO over all fuel types. Figure 2 (right panel) shows a near exponential decrease in ΔOM/ΔCO with a wide range of *f44* from around 0.02 up to 0.30 depending on the stoves and fuel types. A range of ΔOM/ΔCO ratios exhibited an *f44* value lower than 0.05, while ΔOM/ΔCO does not exceed 0.20 when *f44* is greater than 0.05. The dry fuels tended to have a larger value of *f44* compared to wet fuels, indicating that the moisture content of fuel not only affect the magnitude of OM emissions but also the oxidation level of OM.

**BC Core Size.** Figure S7 shows the mass median diameter (MMD) of BC cores as a function of MCE for each experiment. The MMD of average BC mass size distribution for Carbonzero and Gyapa cookstoves show BC core MMD of 188.5 ± 13.6 and 155.1 ± 27.1 nm for dry oak and wet oak, respectively, and these values are independent of MCE ($r$ < 0.1 and 0.4 for Carbonzero and Gyapa cookstoves, respectively). The dependence of MMD on MCE is only found in the heating stove, especially for coal combustion ($r$ = 0.94). This suggests a relatively uniform BC core size for cookstove emissions. The difference of the dependence of MMD on MCE for cookstoves and heating stove may be due to the designs of the stoves, e.g., the heating stove burns fuels in a sealed combustion chamber, whereas the cookstoves are open, thus the residence time of combustion gases in the heating stove may be longer than that in cookstoves, which may cause more significant coagulation of particles in the chamber of the heating stove.

The moisture of fuels only slightly affected the BC core size, such as the MMD of dry oak and willow stick (180.5 ± 18.1 nm), which was slightly larger than that of wet oak (∼160 nm) emissions ($p$-value <0.001). The coal-emitted BC had the largest and widest range of BC core size (223.8 ± 53.8 nm), and its core MMD was strongly correlated with MCE. This may be consistent with the highly positive correlation between the emission ratios of BC and MCE observed for coal, which may result in the strongest self-coagulation effect of BC for coal combustion. BC particles from the heating stove with coal combustion were mostly emitted when MCE > 0.95, so the averaged MMD ≈ 244 nm at MCE > 0.95 was representative for the majority of BC mass from coal combustion. For the Lucia stove, the BC core MMD was ∼190 nm with high MCE, though MMD was ∼100 nm with a minor contribution of total emitted BC mass.

**OM Internally and Externally Mixed with BC-Containing Particles.** The coatings on BC are mainly composed of OM, as sulfate and nitrate only accounted for less than 8% of total mass. Figure S8 shows $F_{in}$ as a function of OM/(OM + BC) and MCE. Except for wet oak, $F_{in}$ shows a significant decrease with OM/(OM+BC) from 0.02 to 0.40 for different fuel types, as shown in Figure S8(a). When OM/(OM + BC) exceeded 0.40, most BC-containing particles comprised less than 40% of the total OM except for a few particles with more than 40% of the total OM. With increasing MCE, $F_{in}$ increased from almost no OM internally mixed with the BC ($F_{in}$ = 0) to nearly all OM coated on BC particles ($F_{in}$ = 1), as shown in Figure S8(b). When MCE was larger than 0.95, a wide range of $F_{in}$ from about 0.1 up to 1 was observed. The positive correlation between $F_{in}$ and MCE implies that during efficient burning, the OM emissions are mostly mixed with high BC emissions. Conversely during periods of inefficient burning when OM emissions are high and there is little BC, nearly all the OM is externally mixed with BC particles. A further comparison was performed with the BC coating measurement (see below) to validate the measurement of OM mixed with BC.

Figure 3 reveals the average $F_{in}$ separated into high (>0.95) and low (<0.95) MCE periods. More than half of the OM was

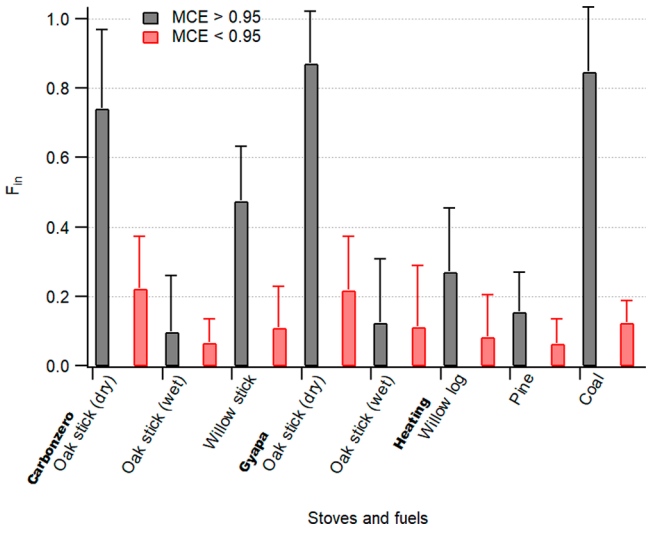


**Figure 3.** Average ratios of internally mixed OM to total OM ($F_{in}$) for each stove and fuel type for MCE > 0.95 and MCE < 0.95. The Lucia stove with pellet fuel is not shown here as the OM was completely coated on the BC particles due to the high BC mass loading and efficient combustion. The error bar shows the standard deviation.

coated on the BC particles when MCE > 0.95 during the dry oak and coal experiments, whereas approximately 20% and 12% of the total OM was coated on the BC when MCE < 0.95 for dry oak and coal, respectively. The fuel with higher moisture tended to have a lower $F_{in}$ at the same MCE compared to drier fuel due to the higher OM emission factors. In the heating stove, the coal combustion has higher $F_{in}$ due to the higher BC mass emission ratio.

**Mixing State of BC.** While the $OM_{BC}/rBC_{bulk}$ ratio does not show consistent correlation with MCE in this study, a certain correlation between the ratio and the OM fraction (OM/(OM + BC)) has been observed, as shown in Figure 4 (left panel). The ratios were mostly lower than 1 when the OM fraction was lower than 0.9; the ratios started to significantly increase when the OM fraction was larger than 0.9, e.g., reaching up to 5 in the cookstoves and 10 for the heating stove. Emissions from the wet fuel had a higher OM fraction than the dry fuel and thus exhibited a higher $OM_{BC}/rBC_{bulk}$ ratio. For an OM fraction larger than 0.9, the $OM_{BC}/rBC_{bulk}$ ratio for the heating stove was much higher than that in the cookstoves, which may be because the dynamics in the enclosed combustion space facilitated the coating process of BC with a higher local concentration of organic vapor.

Figure 4 (right panel) shows that regardless of stoves and fuels, the *f44*/*f43* (*f43*, which the dominant organic ion is $C_2H_3O^+$, denotes the fraction of $m/z$ 43 in the total organic mass spectra) increased with decreased $OM_{BC}/rBC_{bulk}$ ratios in all cases except for the Lucia stove. When the $OM_{BC}/rBC_{bulk}$


DOI: 10.1021/acs.est.8b00456
Environ. Sci. Technol. 2018, 52, 10134−10143

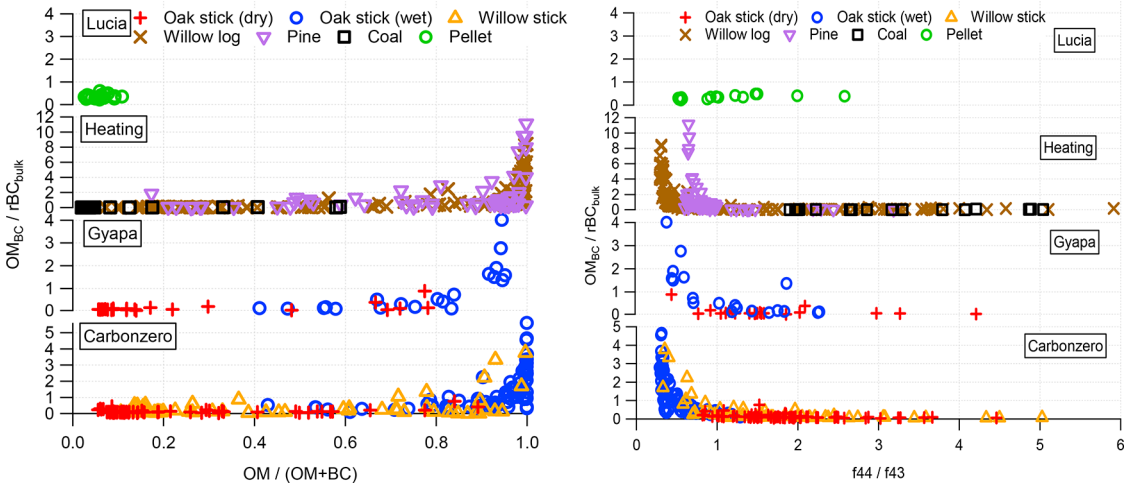


**Figure 4.** $OM_{BC}/rBC_{bulk}$ as a function of the OM/(OM + BC) ratios (left panel). The $OM_{BC}/rBC_{bulk}$ as a function of *f44*/*f43* ratios (right panel).

ratios were lower than 1, there was a wide range of *f44*/*f43* (larger than 1) and the high $OM_{BC}/rBC_{bulk}$ ratios only arose when *f44*/*f43* < 1. As the combustion process for the Lucia stove is different from the others, which have a pyrolysis stage during the combustion cycle, the $OM_{BC}/rBC_{bulk}$ ratio of the Lucia stove emissions shows near constant of below 1 and no relationship with either OM fraction or *f44*/*f43*, suggesting no enhancement of light absorption results from the BC-containing particles emitted from this kind of stove.

## DISCUSSION

With the combination of the AMS and SP2 online measurements, the temporal variability and mixing state of OM and BC over a course of combustion has been observed during different burning phases using a range of cook stoves and fuels. The results here consistently showed an overlap among the phases under the operating conditions unlike those that were observed during more controlled combustion revealing distinguishable burning phases.[31,63] Many studies have used MCE to identify burning phases,[62,63] however the results here show that while trends exist, it is not a complete description, partly because the pyrolysis stage emits large amounts of OM but is not directly represented by a combustion metric.[32]

These experiments found that more complete combustion emitted less OM that was also more oxidized. While *m*/*z* 44 is widely used as an indicator of secondary or aged OM, this shows that primary OM from wood burning exhibits a significant range of *f44*.[27,32] For all the cookstoves tested, negative correlation between *f44* and MCE is shown in Figure 2, consistent with the findings of Weimer et al.[9] In contrast, positive correlations between *f44* and MCE from log and pine combustion were observed in a multifuel heating stove, which may be due to the dominance of hydrocarbon fragments at high MCE. In spite of the difference between *f44* and MCE among the fuel and stove types,[61] a near exponential decline in ΔOM/ΔCO with increased *f44* has been observed in most of the combustion cycles. This is consistent with previous studies where during high MCE, the sufficient supply of oxygen will lead to more oxidation of organics.[61,65] At lower MCEs, the OM emissions were high and the OM was mainly composed of less-oxygenated species, but this differed among fuel types.[61] The relationship between ΔOM/ΔCO and *f44* does show some inconsistency, including the contrasting thresholds between regimes of high and low OM production between different type of fuels and stoves. This is again likely related to the fact that, as found by Haslett et al.,[32] the large emissions from preignition pyrolysis are not related directly to MCE.

The source profile of BC is fundamental to any detailed model when estimating its atmospheric lifetime because mixing state influences loss processes such as in-cloud scavenging. Many global models assume the same BC size for all types of residential solid fuel sources,[37,66] which is consistent with the cookstove data here. However, caution must be taken, as for example, for emissions from the heating stove, the BC core size was dependent on the MCE. The BC concentrations in the heating stove may be important in determining its core size because of the closed combustion chamber. This indicates that combustion in the heating stove during high MCE tends to produce particles with larger BC core size than during low MCE. In general, the intense combustion impedes the efficient transport of oxygen into the flame zone,[67] resulting in the formation of large amounts of small rBC particles. However, since the coagulation rate of particles is approximately proportional to the square of their concentrations,[68] the growth of rBC particles was consequently rapid under high concentrations. In combination with that, the small rBC monomers might easily form agglomerates during high MCE driven by the internally mixed OM when the temperature of flame drops, corresponding to a larger fraction of OM internally mixed with BC. This process may take place in seconds, which occurs too fast to be achievable in ambient measurements.

The mixing state of BC and OM is frequently assumed to be uniform from all sources,[38] and BC is assumed completely externally or internally mixed with coemitted species.[38,69−71] Moreover, the mixing state of BC in models largely relies on the organic carbon (OC)/ elemental carbon (EC)[72] or OM/BC ratio and assumes that all of the coemitted primary OM is internally or externally mixed with BC instantaneously after emission,[70,71] which is likely to overestimate or underestimate the effect of BC-containing particles on radiative forcing.[70] There are numerous different fuels and stoves in actual use emitting BC and OM in potentially different mixing state. However, for the complicated dynamics in burning processes presented, the amount of primary OM emitted as internally or externally mixed with BC shows a certain relationship with MCE. Among combustion events in this study, it was found


DOI: 10.1021/acs.est.8b00456
Environ. Sci. Technol. 2018, 52, 10134−10143

that between 20% and 100% of OM particles contained significant rBC when MCE > 0.95, which should be considered to be internally mixed with BC. When MCE < 0.95, only about 20% of the total OM was internally mixed with BC. These ratios might be useful for improving the accuracy of models in estimating the impact of the mixing state of BC and OM on climate radiative forcing for the regions where the solid fuel combustion from the cookstoves dominates the contributions of carbonaceous species.

The extent to which optical absorption from BC can be theoretically enhanced via lensing, is determined by the mass ratio of non-BC and rBC within a single particle.[35] Liu et al.[35] found that when this ratio was greater than 3, particles displayed an absorption enhancement ($E_{abs}$) of BC. Our results show a certain consistency that when the OM fraction (OM/(OM + BC)) < 0.9, our bulk $OM_{BC}/rBC_{bulk}$ measurement was less than 1 meaning the BC may have not been significantly coated, so would not result in an absorption enhancement. When the OM fraction >0.9, we found $OM_{BC}/rBC_{bulk}$ was often >3, meaning there is more likely to be a BC absorption enhancement from solid fuel combustion. An OM fraction of 0.9 may therefore be used as a threshold value in models to determine whether the absorption enhancement of BC from solid fuel burning will occur or not. The extent to which the absorption is enhanced also depends on the specific fuel type and stove design. The BC emitted from a cookstove may have a lower $E_{abs}$ compared to the heating stove due to the lower $OM_{BC}/rBC_{bulk}$ ratios. In addition to the effect of the amount of the OM emissions, the oxidation level of OM could also be an indicator of the magnitude of the $OM_{BC}/rBC_{bulk}$ based on *f44*/*f43*, which is related to the volatility of oxygenated organic aerosol (OOA).[73] As the non-BC materials in the BC-containing particles mainly comprise OOA,[74] the consistency in the negative correlation between $OM_{BC}/rBC_{bulk}$ and *f44*/*f43* ratios among the fuels suggests that the internally mixed OM is likely to be less oxidized and more semivolatile (low *f44*/*f43*) for those thickly coated BC, consistent with a large fraction of OM being less volatile when OM emission was high (Figure 2).

The correlation of the OM fraction and *f44*/*f43* with $OM_{BC}/rBC_{bulk}$ ratios derived in this study indicates that the ratio of $OM_{BC}$ and $rBC_{bulk}$ from solid fuel emissions depends not only on the OM fraction but also on the oxygenation level of OM. Our results will help to assess the benefits of reduction in BC from cookstoves and so aid mitigation strategies in the future. While this study provides new insight into the combustion processes, we should stress that the results should be treated as indicative for use in models and more authoritative data will require more work, specifically repeat experiments with other fuel types, stove designs and with a more explicit simulation of cooking activity (e.g., inclusion of a cooking pot).

## ■ ASSOCIATED CONTENT

### Supporting Information

The Supporting Information is available free of charge on the ACS Publications website at DOI: 10.1021/acs.est.8b00456.

Additional details of the sampling configuration; the correction for the silicon tubing contamination; table of emission ratios; figures of images of cookstoves; real-time data of dilution factors and emissions of all combustion cycles; total particle number size distribution; BC particle number and mass size distribution; and $F_{in}$ as a function of MCE (PDF)

## ■ AUTHOR INFORMATION


### Corresponding Author

* E-mail: James.Allan@manchester.ac.uk. Phone: +44 (0)161 306 8532.

### ORCID

Yuchieh Ting: 0000-0002-3604-8060
James D. Allan: 0000-0001-6492-4876
Alan Williams: 0000-0002-9841-3203


### Notes

The authors declare no competing financial interest.

## ■ ACKNOWLEDGMENTS

This work has been funded through an EPSRC Pump Priming Grant for Global Challenge Research (grant no. 109602).

## ■ REFERENCES


(1) Dickau, M.; Olfert, J.; Stettler, M. E. J.; Boies, A.; Momenimovahed, A.; Thomson, K.; Smallwood, G.; Johnson, M. Methodology for quantifying the volatile mixing state of an aerosol. *Aerosol Sci. Technol.* **2016**, *50* (8), 759−772.

(2) Lelieveld, J.; Evans, J. S.; Fnais, M.; Giannadaki, D.; Pozzer, A. The contribution of outdoor air pollution sources to premature mortality on a global scale. *Nature* **2015**, *525* (7569), 367−371.

(3) Kodros, J. K.; Scott, C. E.; Farina, S. C.; Lee, Y. H.; L'Orange, C.; Volckens, J.; Pierce, J. R. Uncertainties in global aerosols and climate effects due to biofuel emissions. *Atmos. Chem. Phys.* **2015**, *15* (15), 8577−8596.

(4) Butt, E. W.; Rap, A.; Schmidt, A.; Scott, C. E.; Pringle, K. J.; Reddington, C. L.; Richards, N. A. D.; Woodhouse, M. T.; Ramirez-Villegas, J.; Yang, H.; Vakkari, V.; Stone, E. A.; Rupakheti, M.; Praveen, P. S.; van Zyl, P. G.; Beukes, J. P.; Josipovic, M.; Mitchell, E. J. S.; Sallu, S. M.; Forster, P. M.; Spracklen, D. V. The impact of residential combustion emissions on atmospheric aerosol, human health, and climate. *Atmos. Chem. Phys.* **2016**, *16* (2), 873−905.

(5) Lim, S. S.; Vos, T.; Flaxman, A. D.; Danaei, G.; Shibuya, K.; Adair-Rohani, H.; AlMazroa, M. A.; Amann, M.; Anderson, H. R.; Andrews, K. G.; Aryee, M.; Atkinson, C.; Bacchus, L. J.; Bahalim, A. N.; Balakrishnan, K.; Balmes, J.; Barker-Collo, S.; Baxter, A.; Bell, M. L.; Blore, J. D.; Blyth, F.; Bonner, C.; Borges, G.; Bourne, R.; Boussinesq, M.; Brauer, M.; Brooks, P.; Bruce, N. G.; Brunekreef, B.; Bryan-Hancock, C.; Bucello, C.; Buchbinder, R.; Bull, F.; Burnett, R. T.; Byers, T. E.; Calabria, B.; Carapetis, J.; Carnahan, E.; Chafe, Z.; Charlson, F.; Chen, H.; Chen, J. S.; Cheng, A. T.-A.; Child, J. C.; Cohen, A.; Colson, K. E.; Cowie, B. C.; Darby, S.; Darling, S.; Davis, A.; Degenhardt, L.; Dentener, F.; Des Jarlais, D. C.; Devries, K.; Dherani, M.; Ding, E. L.; Dorsey, E. R.; Driscoll, T.; Edmond, K.; Ali, S. E.; Engell, R. E.; Erwin, P. J.; Fahimi, S.; Falder, G.; Farzadfar, F.; Ferrari, A.; Finucane, M. M.; Flaxman, S.; Fowkes, F. G. R.; Freedman, G.; Freeman, M. K.; Gakidou, E.; Ghosh, S.; Giovannucci, E.; Gmel, G.; Graham, K.; Grainger, R.; Grant, B.; Gunnell, D.; Gutierrez, H. R.; Hall, W.; Hoek, H. W.; Hogan, A.; Hosgood, H. D.; Hoy, D.; Hu, H.; Hubbell, B. J.; Hutchings, S. J.; Ibeanusi, S. E.; Jacklyn, G. L.; Jasrasaria, R.; Jonas, J. B.; Kan, H.; Kanis, J. A.; Kassebaum, N.; Kawakami, N.; Khang, Y.-H.; Khatibzadeh, S.; Khoo, J.-P.; Kok, C.; Laden, F.; Lalloo, R.; Lan, Q.; Lathlean, T.; Leasher, J. L.; Leigh, J.; Li, Y.; Lin, J. K.; Lipshultz, S. E.; London, S.; Lozano, R.; Lu, Y.; Mak, J.; Malekzadeh, R.; Mallinger, L.; Marcenes, W.; March, L.; Marks, R.; Martin, R.; McGale, P.; McGrath, J.; Mehta, S.; Memish, Z. A.; Mensah, G. A.; Merriman, T. R.; Micha, R.; Michaud, C.; Mishra, V.; Hanafiah, K. M.; Mokdad, A. A.; Morawska, L.; Mozaffarian, D.; Murphy, T.; Naghavi, M.; Neal, B.; Nelson, P. K.; Nolla, J. M.; Norman, R.; Olives, C.; Omer, S. B.; Orchard, J.; Osborne, R.; Ostro, B.; Page, A.; Pandey, K. D.; Parry, C. D. H.;




DOI: 10.1021/acs.est.8b00456
*Environ. Sci. Technol.* 2018, 52, 10134−10143

Passmore, E.; Patra, J.; Pearce, N.; Pelizzari, P. M.; Petzold, M.; Phillips, M. R.; Pope, D.; Pope, C. A.; Powles, J.; Rao, M.; Razavi, H.; Rehfuess, E. A.; Rehm, J. T.; Ritz, B.; Rivara, F. P.; Roberts, T.; Robinson, C.; Rodriguez-Portales, J. A.; Romieu, I.; Room, R.; Rosenfeld, L. C.; Roy, A.; Rushton, L.; Salomon, J. A.; Sampson, U.; Sanchez-Riera, L.; Sanman, E.; Sapkota, A.; Seedat, S.; Shi, P.; Shield, K.; Shivakoti, R.; Singh, G. M.; Sleet, D. A.; Smith, E.; Smith, K. R.; Stapelberg, N. J. C.; Steenland, K.; Stöckl, H.; Stovner, L. J.; Straif, K.; Straney, L.; Thurston, G. D.; Tran, J. H.; Van Dingenen, R.; van Donkelaar, A.; Veerman, J. L.; Vijayakumar, L.; Weintraub, R.; Weissman, M. M.; White, R. A.; Whiteford, H.; Wiersma, S. T.; Wilkinson, J. D.; Williams, H. C.; Williams, W.; Wilson, N.; Woolf, A. D.; Yip, P.; Zielinski, J. M.; Lopez, A. D.; Murray, C. J. L.; Ezzati, M. A comparative risk assessment of burden of disease and injury attributable to 67 risk factors and risk factor clusters in 21 regions, 1990−2010: a systematic analysis for the Global Burden of Disease Study 2010. *Lancet* **2012**, *380* (9859), 2224−2260.

(6) WHO. WHO Guidelines for Indoor Air Quality: Household Fuel Combustion. World Health Organization: Geneva, Switzerland. 2014.

(7) Smith, K. R.; Bruce, N.; Balakrishnan, K.; Adair-Rohani, H.; Balmes, J.; Chafe, Z.; Dherani, M.; Hosgood, H. D.; Mehta, S.; Pope, D. Millions dead: how do we know and what does it mean? Methods used in the comparative risk assessment of household air pollution. *Annu. Rev. Public Health* **2014**, *35*, 185−206.

(8) Bond, T. C.; Streets, D. G.; Yarber, K. F.; Nelson, S. M.; Woo, J. H.; Klimont, Z. A technology-based global inventory of black and organic carbon emissions from combustion. *J. Geophys. Res.* **2004**, *109* (D14), D14203.

(9) Weimer, S.; Alfarra, M.; Schreiber, D.; Mohr, M.; Prévôt, A.; Baltensperger, U. Organic aerosol mass spectral signatures from wood-burning emissions: Influence of burning conditions and wood type. *J. Geophys. Res.* **2008**, *113* (D10), D10304.

(10) Jetter, J.; Zhao, Y.; Smith, K. R.; Khan, B.; Yelverton, T.; DeCarlo, P.; Hays, M. D. Pollutant Emissions and Energy Efficiency under Controlled Conditions for Household Biomass Cookstoves and Implications for Metrics Useful in Setting International Test Standards. *Environ. Sci. Technol.* **2012**, *46* (19), 10827−10834.

(11) Bond, T. C.; Doherty, S. J.; Fahey, D.; Forster, P.; Berntsen, T.; DeAngelo, B.; Flanner, M.; Ghan, S.; Kärcher, B.; Koch, D. Bounding the role of black carbon in the climate system: A scientific assessment. *J. Geophys. Res.* **2013**, *118* (11), 5380−5552.

(12) Elsasser, M.; Busch, C.; Orasche, J.; Schön, C.; Hartmann, H.; Schnelle-Kreis, J.; Zimmermann, R. Dynamic changes of the aerosol composition and concentration during different burning phases of wood combustion. *Energy Fuels* **2013**, *27* (8), 4959−4968.

(13) Eriksson, A. C.; Nordin, E. Z.; Nyström, R.; Pettersson, E.; Swietlicki, E.; Bergvall, C.; Westerholm, R.; Boman, C.; Pagels, J. H. Particulate PAH Emissions from Residential Biomass Combustion: Time-Resolved Analysis with Aerosol Mass Spectrometry. *Environ. Sci. Technol.* **2014**, *48* (12), 7143−7150.

(14) Liu, S.; Aiken, A. C.; Gorkowski, K.; Dubey, M. K.; Cappa, C. D.; Williams, L. R.; Herndon, S. C.; Massoli, P.; Fortner, E. C.; Chhabra, P. S.; Brooks, W. A.; Onasch, T. B.; Jayne, J. T.; Worsnop, D. R.; China, S.; Sharma, N.; Mazzoleni, C.; Xu, L.; Ng, N. L.; Liu, D.; Allan, J. D.; Lee, J. D.; Fleming, Z. L.; Mohr, C.; Zotter, P.; Szidat, S.; Prevot, A. S. H. Enhanced light absorption by mixed source black and brown carbon particles in UK winter. *Nat. Commun.* **2015**, *6*, 8435−8435.

(15) Saliba, G.; Subramanian, R.; Saleh, R.; Ahern, A. T.; Lipsky, E. M.; Tasoglou, A.; Sullivan, R. C.; Bhandari, J.; Mazzoleni, C.; Robinson, A. L. Optical properties of black carbon in cookstove emissions coated with secondary organic aerosols: Measurements and modeling. *Aerosol Sci. Technol.* **2016**, *50* (11), 1264−1276.

(16) Flato, G.; Marotzke, J.; Abiodun, B.; Braconnot, P.; Chou, S. C.; Collins, W. J.; Cox, P.; Driouech, F.; Emori, S.; Eyring, V. Evaluation of Climate Models. In: Climate Change 2013: The Physical Science Basis. Contribution of Working Group I to the Fifth Assessment Report of the Intergovernmental Panel on Climate Change. *Climate Change 2013* **2013**, *5*, 741−866.

(17) Venkataraman, C.; Sagar, A. D.; Habib, G.; Lam, N.; Smith, K. R. The Indian National Initiative for Advanced Biomass Cookstoves: The benefits of clean combustion. *Energy Sustainable Dev.* **2010**, *14* (2), 63−72.

(18) Gonçalves, C.; Alves, C.; Evtyugina, M.; Mirante, F.; Pio, C.; Caseiro, A.; Schmidl, C.; Bauer, H.; Carvalho, F. Characterisation of PM10 emissions from woodstove combustion of common woods grown in Portugal. *Atmos. Environ.* **2010**, *44* (35), 4474−4480.

(19) Pettersson, E.; Boman, C.; Westerholm, R.; Boström, D.; Nordin, A. Stove Performance and Emission Characteristics in Residential Wood Log and Pellet Combustion, Part 2: Wood Stove. *Energy Fuels* **2011**, *25* (1), 315−323.

(20) Vicente, E. D.; Duarte, M. A.; Calvo, A. I.; Nunes, T. F.; Tarelho, L. A. C.; Custódio, D.; Colombi, C.; Gianelle, V.; Sanchez de la Campa, A.; Alves, C. A. Influence of operating conditions on chemical composition of particulate matter emissions from residential combustion. *Atmos. Res.* **2015**, *166*, 92−100.

(21) Nyström, R.; Lindgren, R.; Avagyan, R.; Westerholm, R.; Lundstedt, S.; Boman, C. Influence of Wood Species and Burning Conditions on Particle Emission Characteristics in a Residential Wood Stove. *Energy Fuels* **2017**, *31* (5), 5514−5524.

(22) Johansson, L. S.; Tullin, C.; Leckner, B.; Sjövall, P. Particle emissions from biomass combustion in small combustors. *Biomass Bioenergy* **2003**, *25* (4), 435−446.

(23) Pagels, J.; Dutcher, D. D.; Stolzenburg, M. R.; McMurry, P. H.; Gälli, M. E.; Gross, D. S. Fine-particle emissions from solid biofuel combustion studied with single-particle mass spectrometry: Identification of markers for organics, soot, and ash components. *J. Geophys. Res.* **2013**, *118* (2), 859−870.

(24) Shen, G.; Gaddam, C. K.; Ebersviller, S. M.; Vander Wal, R. L.; Williams, C.; Faircloth, J. W.; Jetter, J. J.; Hays, M. D. A Laboratory Comparison of Emission Factors, Number Size Distributions, and Morphology of Ultrafine Particles from 11 Different Household Cookstove-Fuel Systems. *Environ. Sci. Technol.* **2017**, *51* (11), 6522−6532.

(25) Hansen, J.; Sato, M.; Ruedy, R.; Kharecha, P.; Lacis, A.; Miller, R.; Nazarenko, L.; Lo, K.; Schmidt, G. A.; Russell, G.; Aleinov, I.; Bauer, S.; Baum, E.; Cairns, B.; Canuto, V.; Chandler, M.; Cheng, Y.; Cohen, A.; Del Genio, A.; Faluvegi, G.; Fleming, E.; Friend, A.; Hall, T.; Jackman, C.; Jonas, J.; Kelley, M.; Kiang, N. Y.; Koch, D.; Labow, G.; Lerner, J.; Menon, S.; Novakov, T.; Oinas, V.; Perlwitz, J.; Perlwitz, J.; Rind, D.; Romanou, A.; Schmunk, R.; Shindell, D.; Stone, P.; Sun, S.; Streets, D.; Tausnev, N.; Thresher, D.; Unger, N.; Yao, M.; Zhang, S. Climate simulations for 1880−2003 with GISS modelE. *Climate Dynamics* **2007**, *29* (7), 661−696.

(26) L'Orange, C.; Volckens, J.; DeFoort, M. Influence of stove type and cooking pot temperature on particulate matter emissions from biomass cook stoves. *Energy Sustainable Dev.* **2012**, *16* (4), 448−455.

(27) Heringa, M. F.; DeCarlo, P. F.; Chirico, R.; Lauber, A.; Doberer, A.; Good, J.; Nussbaumer, T.; Keller, A.; Burtscher, H.; Richard, A.; Miljevic, B.; Prevot, A. S. H.; Baltensperger, U. Time-Resolved Characterization of Primary Emissions from Residential Wood Combustion Appliances. *Environ. Sci. Technol.* **2012**, *46* (20), 11418−11425.

(28) Just, B.; Rogak, S.; Kandlikar, M. Characterization of Ultrafine Particulate Matter from Traditional and Improved Biomass Cookstoves. *Environ. Sci. Technol.* **2013**, *47* (7), 3506−3512.

(29) Kortelainen, A.; Joutsensaari, J.; Hao, L.; Leskinen, J.; Tiitta, P.; Jaatinen, A.; Miettinen, P.; Sippula, O.; Torvela, T.; Tissari, J.; Jokiniemi, J.; Worsnop, D. R.; Smith, J. N.; Laaksonen, A.; Virtanen, A. Real-Time Chemical Composition Analysis of Particulate Emissions from Woodchip Combustion. *Energy Fuels* **2015**, *29* (2), 1143−1150.

(30) Kar, A.; Rehman, I. H.; Burney, J.; Puppala, S. P.; Suresh, R.; Singh, L.; Singh, V. K.; Ahmed, T.; Ramanathan, N.; Ramanathan, V. Real-Time Assessment of Black Carbon Pollution in Indian



DOI: 10.1021/acs.est.8b00456
*Environ. Sci. Technol.* 2018, 52, 10134−10143

Households Due to Traditional and Improved Biomass Cookstoves. *Environ. Sci. Technol.* **2012**, *46* (5), 2993−3000.
(31) Bruns, E. A.; Krapf, M.; Orasche, J.; Huang, Y.; Zimmermann, R.; Drinovec, L.; Močnik, G.; El-Haddad, I.; Slowik, J. G.; Dommen, J.; Baltensperger, U.; Prévôt, A. S. H. Characterization of primary and secondary wood combustion products generated under different burner loads. *Atmos. Chem. Phys.* **2015**, *15* (5), 2825−2841.
(32) Haslett, S. L.; Thomas, J. C.; Morgan, W. T.; Hadden, R.; Liu, D.; Allan, J. D.; Williams, P. I.; Keita, S.; Liousse, C.; Coe, H. Highly controlled, reproducible measurements of aerosol emissions from combustion of a common African biofuel source. *Atmos. Chem. Phys.* **2018**, *18* (1), 385−403.
(33) Nielsen, I. E.; Eriksson, A. C.; Lindgren, R.; Martinsson, J.; Nyström, R.; Nordin, E. Z.; Sadiktsis, I.; Boman, C.; Nøjgaard, J. K.; Pagels, J. Time-resolved analysis of particle emissions from residential biomass combustion − Emissions of refractory black carbon, PAHs and organic tracers. *Atmos. Environ.* **2017**, *165*, 179−190.
(34) Martinsson, J.; Eriksson, A.; Nielsen, I. E.; Malmborg, V. B.; Ahlberg, E.; Andersen, C.; Lindgren, R.; Nystrom, R.; Nordin, E.; Brune, W. Impacts of combustion conditions and photochemical processing on the light absorption of biomass combustion aerosol. *Environ. Sci. Technol.* **2015**, *49* (24), 14663−14671.
(35) Liu, D.; Whitehead, J.; Alfarra, M. R.; Reyes-Villegas, E.; Spracklen, D. V.; Reddington, C. L.; Kong, S.; Williams, P. I.; Ting, Y.-C.; Haslett, S. Black-carbon absorption enhancement in the atmosphere determined by particle mixing state. *Nat. Geosci.* **2017**, *10* (3), 184−188.
(36) Saliba, G.; Subramanian, R.; Saleh, R.; Ahern, A. T.; Lipsky, E. M.; Tasoglou, A.; Sullivan, R. C.; Bhandari, J.; Mazzoleni, C.; Robinson, A. L. Optical properties of black carbon in cookstove emissions coated with secondary organic aerosols: Measurements and modeling. *Aerosol Sci. Technol.* **2016**, *50* (11), 1264−1276.
(37) Koch, D.; Schulz, M.; Kinne, S.; McNaughton, C.; Spackman, J. R.; Balkanski, Y.; Bauer, S.; Berntsen, T.; Bond, T. C.; Boucher, O.; Chin, M.; Clarke, A.; De Luca, N.; Dentener, F.; Diehl, T.; Dubovik, O.; Easter, R.; Fahey, D. W.; Feichter, J.; Fillmore, D.; Freitag, S.; Ghan, S.; Ginoux, P.; Gong, S.; Horowitz, L.; Iversen, T.; Kirkevaring, G. A.; Klimont, Z.; Kondo, Y.; Krol, M.; Liu, X.; Miller, R.; Montanaro, V.; Moteki, N.; Myhre, G.; Penner, J. E.; Perlwitz, J.; Pitari, G.; Reddy, S.; Sahu, L.; Sakamoto, H.; Schuster, G.; Schwarz, J. P.; Seland, Ø.; Stier, P.; Takegawa, N.; Takemura, T.; Textor, C.; van Aardenne, J. A.; Zhao, Y. Evaluation of black carbon estimations in global aerosol models. *Atmos. Chem. Phys.* **2009**, *9* (22), 9001−9026.
(38) Reddington, C. L.; McMeeking, G.; Mann, G. W.; Coe, H.; Frontoso, M. G.; Liu, D.; Flynn, M.; Spracklen, D. V.; Carslaw, K. S. The mass and number size distributions of black carbon aerosol over Europe. *Atmos. Chem. Phys.* **2013**, *13* (9), 4917−4939.
(39) MacCarty, N.; Still, D.; Ogle, D.; Drouin, T. Assessing cook stove performance: field and lab studies of three rocket stoves comparing the open fire and traditional stoves in Tamil Nadu, India on measures of time to cook, fuel use, total emissions, and indoor air pollution. *Energy Sustainable Dev.* **2008**, http://www.aprovecho.org/web-content/publications/assets/India%20CCT%20Paper_1.7.08.pdf.*14*161
(40) Roden, C. A.; Bond, T. C.; Conway, S.; Osorto Pinel, A. B.; MacCarty, N.; Still, D. Laboratory and field investigations of particulate and carbon monoxide emissions from traditional and improved cookstoves. *Atmos. Environ.* **2009**, *43* (6), 1170−1181.
(41) Preble, C. V.; Hadley, O. L.; Gadgil, A. J.; Kirchstetter, T. W. Emissions and Climate-Relevant Optical Properties of Pollutants Emitted from a Three-Stone Fire and the Berkeley-Darfur Stove Tested under Laboratory Conditions. *Environ. Sci. Technol.* **2014**, *48* (11), 6484−6491.
(42) Lamberg, H.; Sippula, O.; Tissari, J.; Jokiniemi, J. Effects of Air Staging and Load on Fine-Particle and Gaseous Emissions from a Small-Scale Pellet Boiler. *Energy Fuels* **2011**, *25* (11), 4952−4960.
(43) Leskinen, J.; Tissari, J.; Uski, O.; Virén, A.; Torvela, T.; Kaivosoja, T.; Lamberg, H.; Nuutinen, I.; Kettunen, T.; Joutsensaari, J.; Jalava, P. I.; Sippula, O.; Hirvonen, M. R.; Jokiniemi, J. Fine particle emissions in three different combustion conditions of a wood chip-fired appliance − Particulate physico-chemical properties and induced cell death. *Atmos. Environ.* **2014**, *86*, 129−139.
(44) Shen, G.; Chen, Y.; Xue, C.; Lin, N.; Huang, Y.; Shen, H.; Wang, Y.; Li, T.; Zhang, Y.; Su, S.; Huangfu, Y.; Zhang, W.; Chen, X.; Liu, G.; Liu, W.; Wang, X.; Wong, M.-H.; Tao, S. Pollutant Emissions from Improved Coal- and Wood-Fuelled Cookstoves in Rural Households. *Environ. Sci. Technol.* **2015**, *49* (11), 6590−6598.
(45) Mitchell, E. J. S.; Lea-Langton, A. R.; Jones, J. M.; Williams, A.; Layden, P.; Johnson, R. The impact of fuel properties on the emissions from the combustion of biomass and other solid fuels in a fixed bed domestic stove. *Fuel Process. Technol.* **2016**, *142*, 115−123.
(46) $CO_2$Balance Website; www.co2balance.com.
(47) Gyapa Website; http://www.gyapa.com.
(48) World Stove Website; http://worldstove.com/stoves.
(49) Stanley Website; http://www.waterfordstanley.com/stanley-stoves/stanley-stoves/room-heating/solid-fuel.
(50) Lee, T.; Sullivan, A. P.; Mack, L.; Jimenez, J. L.; Kreidenweis, S. M.; Onasch, T. B.; Worsnop, D. R.; Malm, W.; Wold, C. E.; Hao, W. M.; Collett, J. L. Chemical Smoke Marker Emissions During Flaming and Smoldering Phases of Laboratory Open Burning of Wildland Fuels. *Aerosol Sci. Technol.* **2010**, *44* (9), i−v.
(51) Drewnick, F.; Hings, S. S.; DeCarlo, P.; Jayne, J. T.; Gonin, M.; Fuhrer, K.; Weimer, S.; Jimenez, J. L.; Demerjian, K. L.; Borrmann, S.; Worsnop, D. R. A New Time-of-Flight Aerosol Mass Spectrometer (TOF-AMS)—Instrument Description and First Field Deployment. *Aerosol Sci. Technol.* **2005**, *39* (7), 637−658.
(52) Canagaratna, M. R.; Jayne, J. T.; Jimenez, J. L.; Allan, J. D.; Alfarra, M. R.; Zhang, Q.; Onasch, T. B.; Drewnick, F.; Coe, H.; Middlebrook, A.; Delia, A.; Williams, L. R.; Trimborn, A. M.; Northway, M. J.; DeCarlo, P. F.; Kolb, C. E.; Davidovits, P.; Worsnop, D. R. Chemical and microphysical characterization of ambient aerosols with the aerodyne aerosol mass spectrometer. *Mass Spectrom. Rev.* **2007**, *26* (2), 185−222.
(53) McMeeking, G. R.; Hamburger, T.; Liu, D.; Flynn, M.; Morgan, W. T.; Northway, M.; Highwood, E. J.; Krejci, R.; Allan, J. D.; Minikin, A.; Coe, H. Black carbon measurements in the boundary layer over western and northern Europe. *Atmos. Chem. Phys.* **2010**, *10* (19), 9393−9414.
(54) Liu, D.; Flynn, M.; Gysel, M.; Targino, A.; Crawford, I.; Bower, K.; Choularton, T.; Jurányi, Z.; Steinbacher, M.; Hüglin, C.; Curtius, J.; Kampus, M.; Petzold, A.; Weingartner, E.; Baltensperger, U.; Coe, H. Single particle characterization of black carbon aerosols at a tropospheric alpine site in Switzerland. *Atmos. Chem. Phys.* **2010**, *10* (15), 7389−7407.
(55) Bond, T. C.; Bergstrom, R. W. Light Absorption by Carbonaceous Particles: An Investigative Review. *Aerosol Sci. Technol.* **2006**, *40* (1), 27−67.
(56) Liu, D.; Allan, J. D.; Young, D. E.; Coe, H.; Beddows, D.; Fleming, Z. L.; Flynn, M. J.; Gallagher, M. W.; Harrison, R. M.; Lee, J.; Prevot, A. S. H.; Taylor, J. W.; Yin, J.; Williams, P. I.; Zotter, P. Size distribution, mixing state and source apportionment of black carbon aerosol in London during wintertime. *Atmos. Chem. Phys.* **2014**, *14* (18), 10061−10084.
(57) Taylor, J.; Allan, J.; Liu, D.; Flynn, M.; Weber, R.; Zhang, X.; Lefer, B.; Grossberg, N.; Flynn, J.; Coe, H. Assessment of the sensitivity of core/shell parameters derived using the single-particle soot photometer to density and refractive index. *Atmos. Meas. Tech.* **2015**, *8* (4), 1701−1718.
(58) Moteki, N.; Kondo, Y.; Nakamura, S.-i. Method to measure refractive indices of small nonspherical particles: Application to black carbon particles. *J. Aerosol Sci.* **2010**, *41* (5), 513−521.
(59) Turpin, B. J.; Lim, H.-J. Species contributions to PM2. 5 mass concentrations: Revisiting common assumptions for estimating organic mass. *Aerosol Sci. Technol.* **2001**, *35* (1), 602−610.
(60) Symonds, J. Calibration of Fast Response Differential Mobility Spectrometers. *National Physical Lab., Metrology of Airborne Nanoparticles, Standardisation and Applications, London* **2010**. DOI: 10.13140/2.1.2095.1046


DOI: 10.1021/acs.est.8b00456
*Environ. Sci. Technol.* 2018, 52, 10134−10143

(61) Jolleys, M. D.; Coe, H.; McFiggans, G.; McMeeking, G. R.; Lee, T.; Kreidenweis, S. M.; Collett, J. L., Jr.; Sullivan, A. P. Organic aerosol emission ratios from the laboratory combustion of biomass fuels. *J. Geophys. Res.* **2014**, *119* (22), 12850−12871.
(62) Collier, S.; Zhou, S.; Onasch, T. B.; Jaffe, D. A.; Kleinman, L.; Sedlacek, A. J.; Briggs, N. L.; Hee, J.; Fortner, E.; Shilling, J. E.; Worsnop, D.; Yokelson, R. J.; Parworth, C.; Ge, X.; Xu, J.; Butterfield, Z.; Chand, D.; Dubey, M. K.; Pekour, M. S.; Springston, S.; Zhang, Q. Regional Influence of Aerosol Emissions from Wildfires Driven by Combustion Efficiency: Insights from the BBOP Campaign. *Environ. Sci. Technol.* **2016**, *50* (16), 8613−8622.
(63) Corbin, J. C.; Keller, A.; Lohmann, U.; Burtscher, H.; Sierau, B.; Mensah, A. A. Organic Emissions from a Wood Stove and a Pellet Stove Before and After Simulated Atmospheric Aging. *Aerosol Sci. Technol.* **2015**, *49* (11), 1037−1050.
(64) Aiken, A. C.; DeCarlo, P. F.; Kroll, J. H.; Worsnop, D. R.; Huffman, J. A.; Docherty, K. S.; Ulbrich, I. M.; Mohr, C.; Kimmel, J. R.; Sueper, D.; Sun, Y.; Zhang, Q.; Trimborn, A.; Northway, M.; Ziemann, P. J.; Canagaratna, M. R.; Onasch, T. B.; Alfarra, M. R.; Prevot, A. S. H.; Dommen, J.; Duplissy, J.; Metzger, A.; Baltensperger, U.; Jimenez, J. L. O/C and OM/OC Ratios of Primary, Secondary, and Ambient Organic Aerosols with High-Resolution Time-of-Flight Aerosol Mass Spectrometry. *Environ. Sci. Technol.* **2008**, *42* (12), 4478−4485.
(65) Reid, J.; Koppmann, R.; Eck, T.; Eleuterio, D. A review of biomass burning emissions part II: intensive physical properties of biomass burning particles. *Atmos. Chem. Phys.* **2005**, *5* (3), 799−825.
(66) Dentener, F.; Kinne, S.; Bond, T.; Boucher, O.; Cofala, J.; Generoso, S.; Ginoux, P.; Gong, S.; Hoelzemann, J.; Ito, A. Emissions of primary aerosol and precursor gases in the years 2000 and 1750 prescribed data-sets for AeroCom. *Atmos. Chem. Phys.* **2006**, *6* (12), 4321−4344.
(67) Jones, J. M.; Lea-Langton, A. R.; Ma, L.; Pourkashanian, M.; Williams, A. *Pollutants Generated by the Combustion of Solid Biomass Fuels*. 2014.
(68) Lee, K. W.; Chen, H. Coagulation Rate of Polydisperse Particles. *Aerosol Sci. Technol.* **1984**, *3* (3), 327−334.
(69) Wang, Y.; Wang, M.; Zhang, R.; Ghan, S. J.; Lin, Y.; Hu, J.; Pan, B.; Levy, M.; Jiang, J. H.; Molina, M. J. Assessing the effects of anthropogenic aerosols on Pacific storm track using a multiscale global climate model. *Proc. Natl. Acad. Sci. U. S. A.* **2014**, *111* (19), 6894−6899.
(70) Klingmüller, K.; Steil, B.; Brühl, C.; Tost, H.; Lelieveld, J. Sensitivity of aerosol radiative effects to different mixing assumptions in the AEROPT 1.0 submodel of the EMAC atmospheric-chemistry−climate model. *Geosci. Model Dev.* **2014**, *7* (5), 2503−2516.
(71) Wiedinmyer, C.; Akagi, S.; Yokelson, R. J.; Emmons, L.; Al-Saadi, J.; Orlando, J.; Soja, A. The Fire INventory from NCAR (FINN): a high resolution global model to estimate the emissions from open burning. *Geosci. Model Dev.* **2011**, *4* (3), 625.
(72) Turpin, B. J.; Saxena, P.; Andrews, E. Measuring and simulating particulate organics in the atmosphere: problems and prospects. *Atmos. Environ.* **2000**, *34* (18), 2983−3013.
(73) Ng, N. L.; Canagaratna, M. R.; Zhang, Q.; Jimenez, J. L.; Tian, J.; Ulbrich, I. M.; Kroll, J. H.; Docherty, K. S.; Chhabra, P. S.; Bahreini, R.; Murphy, S. M.; Seinfeld, J. H.; Hildebrandt, L.; Donahue, N. M.; DeCarlo, P. F.; Lanz, V. A.; Prévôt, A. S. H.; Dinar, E.; Rudich, Y.; Worsnop, D. R. Organic aerosol components observed in Northern Hemispheric datasets from Aerosol Mass Spectrometry. *Atmos. Chem. Phys.* **2010**, *10* (10), 4625−4641.
(74) Cappa, C. D.; Onasch, T. B.; Massoli, P.; Worsnop, D. R.; Bates, T. S.; Cross, E. S.; Davidovits, P.; Hakala, J.; Hayden, K. L.; Jobson, B. T.; Kolesar, K. R.; Lack, D. A.; Lerner, B. M.; Li, S.-M.; Mellon, D.; Nuaaman, I.; Olfert, J. S.; Petäjä, T.; Quinn, P. K.; Song, C.; Subramanian, R.; Williams, E. J.; Zaveri, R. A. Radiative Absorption Enhancements Due to the Mixing State of Atmospheric Black Carbon. *Science* **2012**, *337* (6098), 1078−1081.


DOI: 10.1021/acs.est.8b00456
*Environ. Sci. Technol.* 2018, 52, 10134−10143